

RD-A128 634

MODIFICATION OF MUSAT AEROTRIANGULATION PROGRAMS TO  
ACCOMMODATE BATHYMETRIC IMAGE POINTS(U) AUTOMETRIC INC  
FALLS CHURCH VA S R LAMBERT MAY 83 ETL-0306

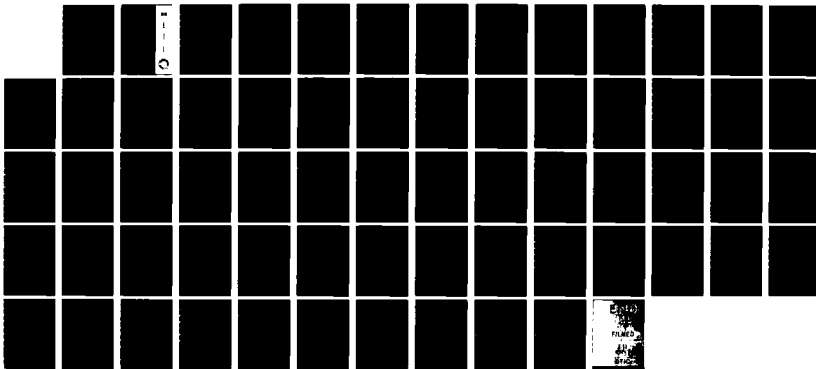
1/1

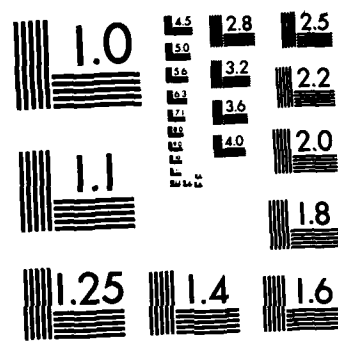
UNCLASSIFIED

DRAK70-79-C-0158

F/G 8/10

NL





MICROCOPY RESOLUTION TEST CHART  
NATIONAL BUREAU OF STANDARDS-1963-A

(2)

ETL-0306

AD A 128634

Modification of MUSAT  
aerotriangulation programs to  
accommodate bathymetric  
image points

Steven R. Lambert

AUTOMETRIC Inc.  
5205 Leesburg Pike  
Suite 1308, Skyline 1  
Falls Church, VA 22041

MAY 1983



DTIC FILE COPY

Prepared For  
U.S. ARMY CORPS OF ENGINEERS  
ENGINEER TOPOGRAPHIC LABORATORIES  
FORT BELVOIR, VIRGINIA 22060



E

T

L

Destroy this report when no longer needed.  
Do not return it to the originator.

---

The findings in this report are not to be construed as an official  
Department of the Army position unless so designated by other  
authorized documents.

---

The citation in this report of trade names of commercially available  
products does not constitute official endorsement or approval of the  
use of such products.

**UNCLASSIFIED**

SECURITY CLASSIFICATION OF THIS PAGE (When Data Entered)

REPORT DOCUMENTATION PAGE		READ INSTRUCTIONS BEFORE COMPLETING FORM
1. REPORT NUMBER ETL-806	2. GOVT ACCESSION NO. AD-A128634	3. RECIPIENT'S CATALOG NUMBER
4. TITLE (and Subtitle) Modification of the MUSAT Aerotriangulation Programs to Accommodate Bathymetric Image Points		5. TYPE OF REPORT & PERIOD COVERED Final Report
7. AUTHOR(s) Steven R. Lambert	6. PERFORMING ORG. REPORT NUMBER DAAK70-79-C-0158	
9. PERFORMING ORGANIZATION NAME AND ADDRESS Autometric Inc. 5205 Leesburg Pike Suite 1308 Falls Church, Virginia 22041	10. PROGRAM ELEMENT, PROJECT, TASK AREA & WORK UNIT NUMBERS Project R4302 Task 0B Work Unit 26	
11. CONTROLLING OFFICE NAME AND ADDRESS U. S. Army Engineer Topographic Laboratories Fort Belvoir, Virginia 22060	12. REPORT DATE May 1983	
14. MONITORING AGENCY NAME & ADDRESS (if different from Controlling Office)	13. NUMBER OF PAGES 62	
15. SECURITY CLASS. (of this report) UNCLASSIFIED		
16. DISTRIBUTION STATEMENT (of this Report)  Approved for public release; distribution unlimited.		
17. DISTRIBUTION STATEMENT (of the abstract entered in Block 20, if different from Report)		
18. SUPPLEMENTARY NOTES		
19. KEY WORDS (Continue on reverse side if necessary and identify by block number) Bathymetric triangulation MUSAT-IIA Bathymetric mapping MUSAT-III Bathymetric data collection AS-11 compilation		
20. ABSTRACT (Continue on reverse side if necessary and identify by block number) This Final Report presents the results of the modifications to the MUSAT aerotriangulation programs to accommodate bathymetric image points. This report develops the mathematical models for the two-media refraction problem encountered in bathymetric mapping. This report also presents the results of the modification of the AS-11 frame compilation program for the compilation of bathymetric data. The modified programs have been installed and tested at DMAH/TC, Washington, D.C.		

TABLE OF CONTENTS

		<u>PAGE</u>
1.0	INTRODUCTION	1
2.0	THEORY OF MULTI-MEDIA REFRACTION	4
3.0	MUSAT-IIA	
3.1	Derivation of Mathematical Model for Refraction Correction	7
3.2	Description of New Subroutine	15
3.3	Dictionary of New Common Blocks	18
4.0	MUSAT-III A	
4.1	Derivation of Mathematical Model for Refraction Correction	19
4.2	Description of New Subroutines	28
4.3	Dictionary of New Common Blocks	35
5.0	MODIFICATION OF AS-11AM FRAME SOFTWARE FOR BATHYMETRIC COMPILATION	
5.1	Computation of True Coordinates for Bathymetric Points	37
6.0	TESTING AND EVALUATION OF MODIFIED MUSAT AND AS-11 PROGRAMS	41

### LIST OF FIGURES

<u>Figure No.</u>	<u>Title</u>	<u>Page</u>
2.1	Snell's Law of Refraction	4
2.2	Effects of Refraction on a Stereo Model	5
3.1	Multiple Ray Intersection for a Bathymetric Point	12
4.1	Refraction in a Bathymetric Point Image	20
4.2	Top View Bathymetric Image Ray	22

Accession For	
NTIS GRA&I	<input checked="" type="checkbox"/>
DTIC TAB	<input type="checkbox"/>
Unannounced	<input type="checkbox"/>
Justification	
By _____	
Distribution/ _____	
Availability Codes	
Dist	Avail and/or Special
A	



LIST OF TABLES

<u>Table No.</u>	<u>Title</u>	<u>Page</u>
6.1	Camera Station Position Analysis Standard MUSAT-IIA	46
6.2	Camera Station Attitude Analysis Standard MUSAT-IIA	47
6.3	Ground Point Analysis Standard MUSAT-IIA	48
6.4	Plate Residuals Standard MUSAT-IIA	49
6.5	Camera Station Position Analysis Modified MUSAT-IIA	50
6.6	Camera Station Attitude Analysis Modified MUSAT-IIA	51
6.7	Ground Point Analysis Modified MUSAT-IIA	52
6.8	Plate Residuals Modified MUSAT-IIA	53
6.9	Comparison of Computed Bathymetric Point Coordinates	54

## PREFACE

This report is generated under Contract DAAK70-79-C-0158 for the U.S. Army Engineer Topographic Laboratories, Fort Belvoir, Virginia 22060, by Autometric, Inc., Falls Church, Virginia, and submitted as ETL-0306. The Contract Officer's Representatives were Mr. John Armistead and Mr. Eugene Taylor.

## 1.0

INTRODUCTION

The objective of this effort is to mathematically model the two media refraction process and incorporate this model into the existing MUSAT aerotriangulation programs. This will permit these revised programs to accomodate photographic image points that appear in shallow water as well as those which appear above the surface.

Classic hydrographic mapping in shoal waters using surface vessels is hazardous, costly, and very time consuming. Precision three-dimensional photogrammetric techniques offer a basic alternative which minimizes these drawbacks. Single stereophotogrammetric models are currently being oriented in analog plotters for the compilation of depth curves and bathymetric features. However, this can only be done where sufficient control exists to scale and orient the model. Photogrammetric aerotriangulation techniques currently in use would appear to satisfy the need for control densification in bathymetric models. With the mathematical model in place, large blocks of overlapping aerial photographs can be used to map extensive offshore shoal areas.

In considering the development of the math model to correct for refraction, the following assumptions have been made:

- a. The elevation of the water surface is known from tidal data, for each exposure.
- b. The wave induced refraction effects will result in plate residuals and ground point errors which are uncorrectable in this effort.
- c. Light rays reflected from a bottom feature travel in a straight line while in the water.
- d. As a result of these assumptions, there will be some

discrepancies which cannot be accounted for. Within reason, these will be included in the normal plate residuals.

This final report presents the results of the modifications to the MUSAT aerotriangulation programs to accommodate bathymetric image points, as contracted by USAMERADCOM. Two versions of the MUSAT programs were modified, MUSAT-IIA, and MUSAT-III A. These two programs use different theory in their solution algorithms and therefore warrant different approaches to the multi-media refraction problem incurred by bathymetric points.

The MUSAT-IIA software package utilizes the theory of modified geodetic restraint. Under this theory, only camera station parameters (attitude and position) are considered unknown. The collinearity condition equations are then written for all control points whether fully known or not. Coplanarity and scale restraint are then applied to all pass points. Equal elevation and known airbase conditions can also be enforced.

The MUSAT-III A program performs a simultaneous block solution using all points. Collinearity condition equations are written for all points, whether fully known or not. The system of equations is solved simultaneously for all point coordinates. Consequently, the water refraction corrections must be applied to the observed image coordinates for every iteration of the simultaneous solution.

The remainder of the report discusses the changes to the input requirements and output formats for the bathymetric solution for both MUSAT-IIA and MUSAT-III A. The modifications to the existing AS-11AM software to allow compilation of subsurface information are also presented.

All programming changes and additions to the MUSAT programs are written in FORTRAN for implementation on DMA/HTC Univac 1108 under the EXEC 8 operating system. Program changes to the AS-11AM software are written in FORTRAN for implementation on the MODCOMP II/25 under the MAX III operating system.

From a photogrammetric standpoint, the effect of refraction due to the water column above a submerged point, is a displacement of the point's image on a photograph. The submerged point's image is displaced radially outward from the principal point. The magnitude of the displacement is a function of the spatial relationship existing between: the exposure station attitude and position, the submerged point, and the height of the water surface, at the time of exposure.

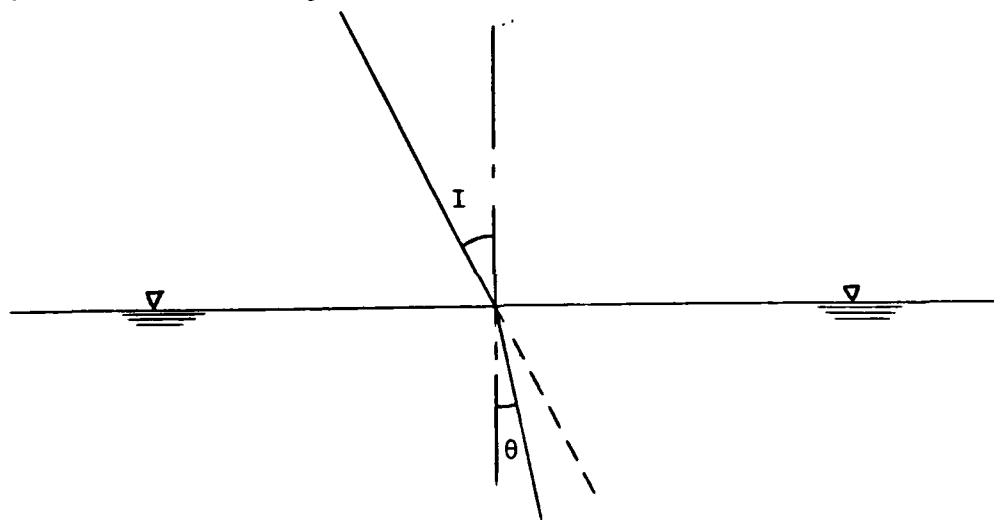


Figure 2.1 Snell's Law of Refraction

The law may be stated as:

$$\sin \theta = \frac{\sin I}{n}$$

where:

n

- Refractive index at the interface

I

- Angle of incidence of the image ray

θ

- Angle of refraction of the image ray

It is appropriate at this point to stress that no attempt was made to model the effects of wave action and that all refractive corrections assume a smooth surface. Figure 2.2 illustrates the effect of water refraction in a stereo model.

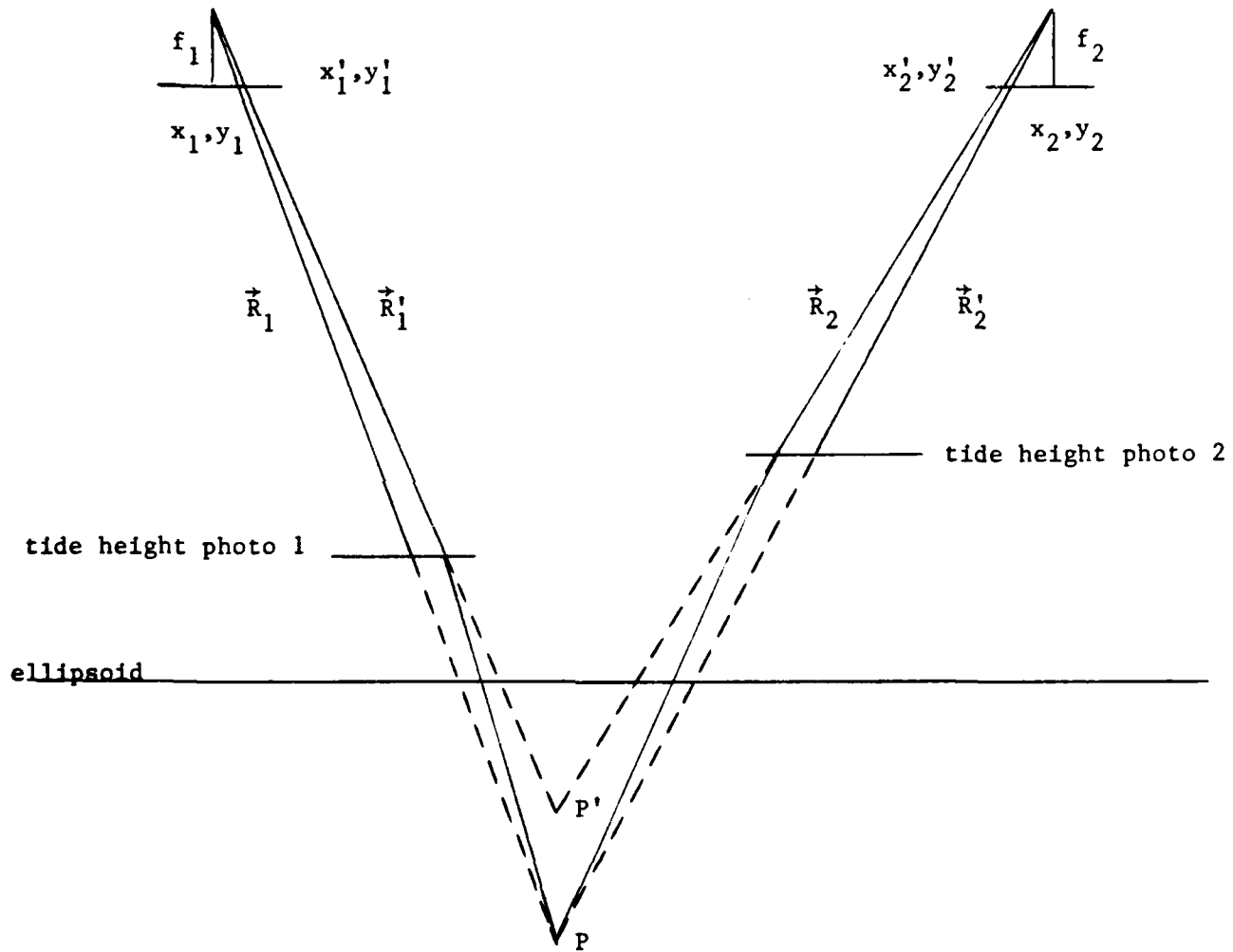


Figure 2.2 Effects of Refraction on a Stereo Model

$f_1, f_2$	- Focal lengths for each photograph
$x'_1, y'_1, x'_2, y'_2$	- Image coordinates of the apparent underwater point on each photograph
$x_1, y_1, x_2, y_2$	- Image coordinates of the true underwater point
$\hat{R}'_1, \hat{R}'_2$	- Image rays in space of the apparent underwater point
$\hat{R}_1, \hat{R}_2$	- Image rays in space of the true underwater point
$P'$	- Apparent position of the underwater point
$P$	- True position of the underwater point

In Figure 2.2, the values of  $x_1, y_1, x_2, y_2$ , are the corrected image coordinates after the refraction model has been applied. Note, that in order to accommodate submerged points for both versions of MUSAT, all triangulation data must be referenced to the ellipsoid. That is, all exposure station attitudes and positions, and all ground point positions must be in a geographic ( $\phi, \lambda, h$ ), or geocentric (X, Y, Z) coordinate system.

At this point, we can begin the derivation of the mathematical models for refraction. As noted earlier, due to the differences between MUSAT-IIA and MUSAT-III A, different models are required for each version. Each will be derived independently to retain clarity.

## 3.1

Derivation of Mathematical Model for Refraction Correction

The first step in the algorithm concerns the establishment of a local vertical coordinate system sufficiently near the submerged points' position so as to not be affected by earth curvature. The following notation convention is established:

$X_i, Y_i, Z_i$	- Camera station "i" geocentric position
$M_i$	- Camera to geocentric rotation matrix for exposure station "i"
$f_i$	- Focal length of camera "i"
$x'_i, y'_i$	- Image coordinates of an apparent submerged point on photograph "i"
$X_p', Y_p', Z_p'$	- Geocentric position of point P'

The collinearity condition is:

$$\begin{bmatrix} X - X_i \\ Y - Y_i \\ Z - Z_i \end{bmatrix} = k_i M_i \begin{bmatrix} x'_i \\ y'_i \\ f_i \end{bmatrix} = k_i \hat{R}'_i \quad (3.1)$$

where:

$k_i$	- Scale factor
$\hat{R}'_i$	- Object space image ray corresponding to the apparent position of the submerged point.

(It is assumed that the focal length carries the proper algebraic sign)

By intersecting the image rays from the first two exposure stations, we can define an appropriate origin for a local vertical coordinate system. The mathematics for this intersection are:

$$k_1 = \frac{(\vec{d} \times \vec{b}) \cdot \vec{r}_2'}{(\vec{d} \cdot \vec{d})} \quad (3.2)$$

$$k_2 = \frac{(\vec{d} \times \vec{b}) \cdot \vec{r}_1'}{(\vec{d} \cdot \vec{d})} \quad (3.3)$$

$$\vec{d} = \vec{r}_1' \times \vec{r}_2' \quad (3.4)$$

$$\vec{b} = \begin{bmatrix} x_2 - x_1 \\ y_2 - y_1 \\ z_2 - z_1 \end{bmatrix} \quad (3.5)$$

$$\begin{bmatrix} x_{p'} \\ y_{p'} \\ z_{p'} \end{bmatrix} = \frac{1}{2} \begin{bmatrix} x_1 \\ y_1 \\ z_1 \end{bmatrix} + k_1 \vec{r}_1' + \begin{bmatrix} x_2 \\ y_2 \\ z_2 \end{bmatrix} + k_2 \vec{r}_2' \quad (3.6)$$

We can now convert the geocentric coordinates of the point  $P'$  into geographic coordinates  $(\phi_{p'}, \lambda_{p'}, h_{p'})$ . Also, the local-to-geocentric orientation matrix ( $\bar{M}$ ) can be formed. This matrix takes the form:

$$\bar{M} = \begin{bmatrix} -\sin \lambda_{p'} & -\sin \phi_{p'} \cos \lambda_{p'} & \cos \phi_{p'} \cos \lambda_{p'} \\ \cos \lambda_{p'} & -\sin \phi_{p'} \sin \lambda_{p'} & \cos \phi_{p'} \sin \lambda_{p'} \\ 0 & \cos \phi_{p'} & \sin \phi_{p'} \end{bmatrix} \quad (3.7)$$

This orientation matrix defines a local system in which the "Z" axis is the local vertical. Making  $P'$  the origin of the local system, the transformation from local to geocentric is now:

$$\begin{bmatrix} x - x_{p'} \\ y - y_{p'} \\ z - z_{p'} \end{bmatrix} = \bar{M} \begin{bmatrix} \bar{x} \\ \bar{y} \\ \bar{z} \end{bmatrix} \quad (3.8)$$

where:

$x, y, z$  - Geocentric coordinates of a point

$\bar{x}, \bar{y}, \bar{z}$  - Local coordinates of the point

The next task is to compute the point of intersection of all image rays for the submerged point (not just those on the first two photographs) with the water surface. Using equations (3.8) and (3.1) the expression for the conversion of an image ray to the local system is:

$$\begin{bmatrix} X_1 \\ Y_1 \\ Z_1 \end{bmatrix} + k_1 \bar{M}_1 \begin{bmatrix} x'_1 \\ y'_1 \\ f_1 \end{bmatrix} = \begin{bmatrix} X_{P'} \\ Y_{P'} \\ Z_{P'} \end{bmatrix} + \bar{M} \begin{bmatrix} \bar{x} \\ \bar{y} \\ \bar{z} \end{bmatrix} \quad (3.9)$$

Or,

$$\begin{bmatrix} \bar{x} \\ \bar{y} \\ \bar{z} \end{bmatrix} = \bar{M}^T \begin{bmatrix} X_1 - X_{P'} \\ Y_1 - Y_{P'} \\ Z_1 - Z_{P'} \end{bmatrix} = k_1 \bar{M}^T M_1 \begin{bmatrix} x'_1 \\ y'_1 \\ f_1 \end{bmatrix} \quad (3.10)$$

Further substitution yields a compact solution for the object space image ray at exposure station "i" in the local coordinate system:

$$\begin{bmatrix} \bar{x} \\ \bar{y} \\ \bar{z} \end{bmatrix} = \begin{bmatrix} \bar{x}_1 \\ \bar{y}_1 \\ \bar{z}_1 \end{bmatrix} + k_1 \bar{M}^T \bar{r}_1 = \begin{bmatrix} \bar{x}_1 \\ \bar{y}_1 \\ \bar{z}_1 \end{bmatrix} + k_1 \bar{r}_1 \quad (3.11)$$

where:

- $\bar{x}_1, \bar{y}_1, \bar{z}_1$  - Local coordinates of exposure station "i"
- $\bar{r}_1$  - Direction numbers of object space image ray "i" in the local system
- $\bar{x}, \bar{y}, \bar{z}$  - Terminus of the object space image ray in the local system

The intersection of object space ray "i" with the water surface can now be defined by assigning " $\bar{z}$ " a value equal to the tide elevation associated with photograph "i", in the local coordinate system. Therefore, let:

$$\bar{z}_{w_i} = h_{t_i} - h_{p'} \quad (3.12)$$

where:

$h_{t_1}$  - Geographic height of the tidal surface.

Equations (3.11) and (3.12) are combined to yield a solution for the water surface intersection:

$$\begin{aligned}\bar{x}_{w_1} &= \bar{x}_i + (h_t - h_{p_1} - \bar{z}_i) (r_1/r_3) \\ \bar{y}_{w_1} &= \bar{y}_i + (h_t - h_{p_1} - \bar{z}_i) (r_2/r_3)\end{aligned}\quad (3.13)$$

where:

$r_1, r_2, r_3$  - Elements of the direction number vector  $\bar{r}_1$

$\bar{x}_{w_1}, \bar{y}_{w_1}$  - Local coordinates of the water surface intersection

The Law of Refraction is now applied to each object space ray by first computing the angle of incidence of the ray and then determining the angle of refraction. This is done using the following expressions:

$$\tan(I_i) = \frac{\bar{d}_i}{\bar{z}_i - (h_{t_1} - h_{p_1})} \quad (3.14)$$

$$\bar{d}_i = ((\bar{x}_i - \bar{x}_{w_1})^2 + (\bar{y}_i - \bar{y}_{w_1})^2)^{1/2} \quad (3.15)$$

$$\theta_i = \sin^{-1} \left[ \frac{\sin(I_i)}{n} \right] \quad (3.16)$$

The object space ray under the water surface can now be determined for each incident ray by:

$$\vec{u}_i = \begin{bmatrix} \frac{(h_{t_i} - h_{p'}) \tan(\theta_i) (\bar{x}_{w_i} - \bar{x}_i)}{\bar{d}_i} \\ \frac{(h_{t_i} - h_{p'}) \tan(\theta_i) (\bar{y}_{w_i} - \bar{y}_i)}{\bar{d}_i} \\ -(h_{t_i} - h_{p'}) \end{bmatrix} \quad (3.17)$$

where:

$\vec{u}_i$  - Underwater object space ray in the local coordinate system

We now have the situation depicted in Figure 3.1. With "m" image points we can form "m" underwater object space rays " $\vec{u}_i$ ". A new estimate of the submerged point's position,  $P'$ , can be determined by the intersection of all the rays. The equations required take the form of the collinearity condition:

$$\begin{bmatrix} \bar{x}_{p''} - \bar{x}_{w_i} \\ \bar{y}_{p''} - \bar{y}_{w_i} \\ \bar{z}_{p''} - \bar{z}_{w_i} \end{bmatrix} = k_i \cdot \vec{u}_i \quad (3.18)$$

A quick, and sufficiently rigorous intersection can be performed by rearranging equation (3.18) to become:

$$\begin{aligned} \bar{x}_{p''} &= (u_1/u_3)_i (\bar{z}_{p''}) = \bar{x}_{w_i} - (u_1/u_3)_i (\bar{z}_{w_i}) \\ \bar{y}_{p''} &= (u_2/u_3)_i (\bar{z}_{p''}) = \bar{y}_{w_i} - (u_2/u_3)_i (\bar{z}_{w_i}) \end{aligned} \quad (3.19)$$

where:

$u_1, u_2, u_3$  - Elements of the underwater object space ray " $\vec{u}_i$ "

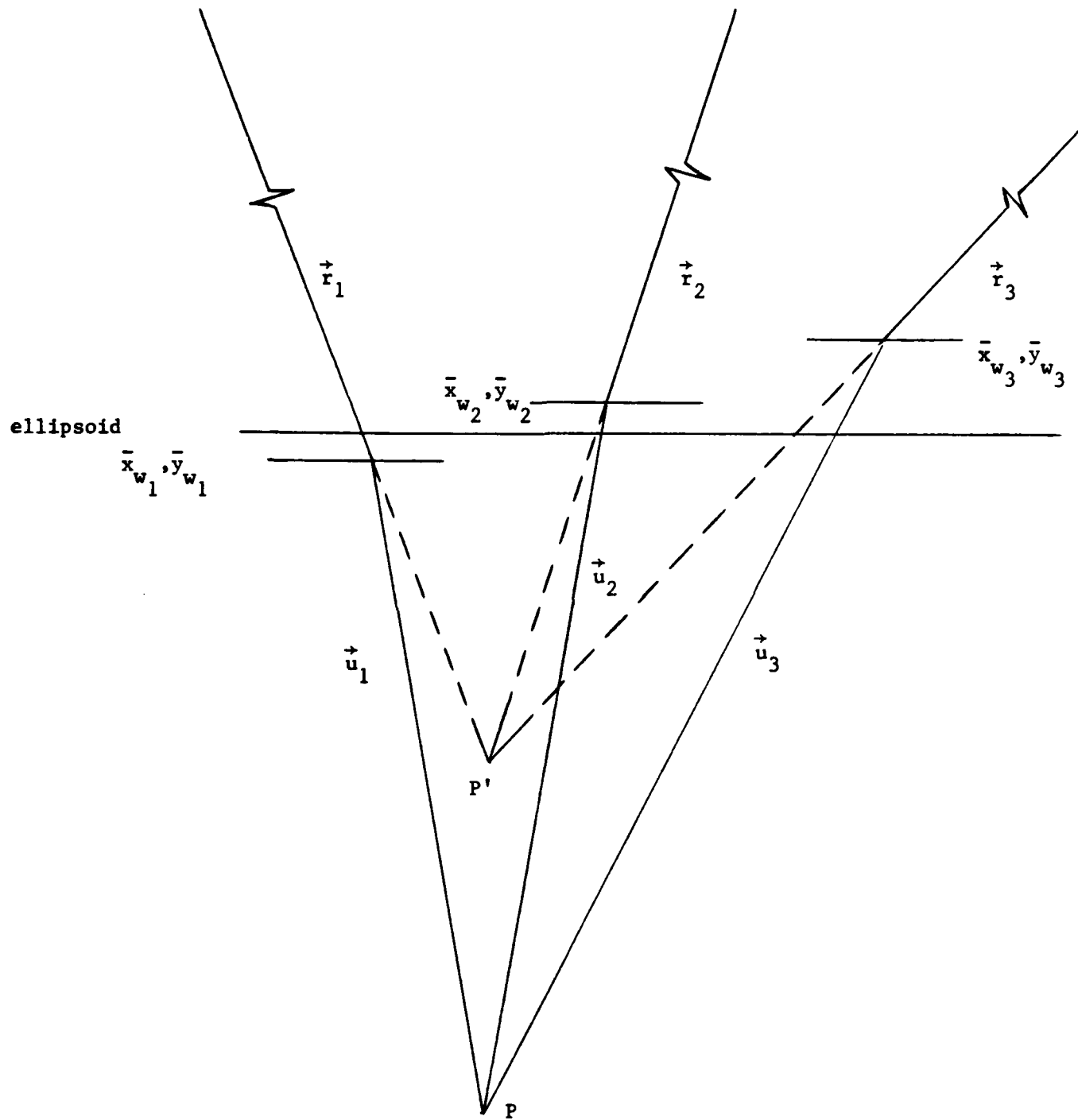


Figure 3.1 Multiple Ray Intersection for a Bathymetric Point.

The result is the following system of equations for all object space rays for the submerged point:

$$\begin{bmatrix} 1 & 0 & -(u_1/u_3)_1 \\ 0 & 1 & -(u_2/u_3)_1 \\ \vdots & \vdots & \vdots \\ 0 & 1 & -(u_2/u_3)_m \end{bmatrix} \begin{bmatrix} \bar{x}_{p''} \\ \bar{y}_{p''} \\ \bar{z}_{p''} \end{bmatrix} = \begin{bmatrix} \bar{x}_{w_1} - (u_1/u_3)_1(\bar{z}_{w_1}) \\ \bar{y}_{w_1} - (u_2/u_3)_1(\bar{z}_{w_1}) \\ \vdots \\ \bar{x}_{w_1} - (u_1/u_3)_m(\bar{z}_{w_1}) \\ \bar{y}_{w_1} - (u_2/u_3)_m(\bar{z}_{w_1}) \end{bmatrix} \quad (3.20)$$

The solution of this system of equations yields a new estimate of the position of the submerged point  $P''$ , in the local system. The new coordinates may be converted to geocentric by:

$$\begin{bmatrix} x_{p''} \\ y_{p''} \\ z_{p''} \end{bmatrix} = \begin{bmatrix} x_{p'} \\ y_{p'} \\ z_{p'} \end{bmatrix} + \bar{M} \begin{bmatrix} \bar{x}_{p''} \\ \bar{y}_{p''} \\ \bar{z}_{p''} \end{bmatrix} \quad (3.21)$$

The final step of the algorithm is to determine a new set of image coordinates for each image of the submerged points. The image coordinates are computed by rearranging the collinearity condition equations:

$$x_i = f_i \frac{m_i}{q_i} \quad (3.22)$$

$$y_i = f_i \frac{n_i}{q_i} \quad (3.23)$$

$$m_1 = m_{11}(X_{P''} - X_1) + m_{12}(Y_{P''} - Y_1) + m_{13}(Z_{P''} - Z_1) \quad (3.24)$$

$$n_1 = m_{21}(X_{P''} - X_1) + m_{22}(Y_{P''} - Y_1) + m_{23}(Z_{P''} - Z_1) \quad (3.25)$$

$$q_1 = m_{31}(X_{p''} - X_1) + m_{32}(Y_{p''} - Y_1) + m_{33}(Z_{p''} - Z_1) \quad (3.26)$$

where:

$$m_{11} = m_{33}$$

- Elements of the camera to geocentric rotation matrix

$$x_i, \quad y_i$$

- New image coordinates of the submerged point based on the updated (true) position of the submerged point

It can be shown that as the difference in position of the points  $P'$  and  $P''$  becomes negligibly small, that  $P''$  actually approaches the true position of the submerged point,  $P$ . This criteria will be used to test for convergence of the water point correction solution.

## 3.2

Description of New Subroutine

A new subroutine has been incorporated into the MUSAT-IIA aerotriangulation software package. It corrects the observed image coordinates of an apparent submerged point to reflect its true position. Subroutine WATPT is engaged only when a submerged point is encountered in the input data for a triangulation run. Should there be no submerged points, its inclusion will in no way affect the solution of a standard job.

3.2.1 SUBROUTINE WATPT

SUBROUTINE: WATPT

DATE WRITTEN: November 1980

LANGUAGE/MACHINE: FORTRAN / UNIVAC 1108 Exec 8

DESCRIPTION: This routine corrects the observed image coordinates of a bathymetric point to reflect it's true position.

CALL LINE: Call WATPT

INPUT: Thru ITAPE3:

GNDINF - Image point records

OUTPUT: Thru ITAPE2:

GNDINF - Image point records with new estimates for the image coordinates

METHOD: As stated earlier, the image coordinates corrections are made to a pre-triangulated data set, and therefore estimates exist for all camera and ground point parameters. The routine cycles through each physical point record and skips it if no submerged point is found. Upon locating a point record for a submerged point the following operations take place.

First, a local vertical coordinate system is established at the intersection of the image rays of the submerged point from the first two photographs on which the point appears. Then, the image rays from all photographs on which the point appears are intersected to produce a better estimate of the point's position. All relevant parameters are now transformed into the local vertical system, including the tidal elevation. The resulting coordinates for the submerged point are transformed into the geocentric coordinate system.

At this point, updated image coordinates are computed for each image of the submerged point, reflecting the effect of the change in the point's position on its corresponding images. These corrected image coordinates and submerged point coordinates are written out to the physical point record. This process is repeated for each submerged point encountered as the routine cycles through the physical point records.

**LIMITATIONS:**       NONE

**COMMON BLOCKS:**    /WATER/    /TAPES/    /CAMDAT/  
                      /AXES/    /TOTAL/

**OPTIONS:**           NONE

**SUBROUTINES  
REFERENCED:**       Function BIGM, MPYAB, SUBMAT, ADDMAT, CROSS, DOT, XYZPLH,  
                      ROTFRM, INVRT

## COMMON /WATER/ IWTPT, REFIDX

<u>VARIABLE</u>	<u>TYPE</u>	<u>DESCRIPTION</u>
IWTPT	Integer	Bathymetric points flag
		0 = No bathymetric points this job 1 = Bathymetric points in this job
REFIDX	Real	Index of refraction of the water body
		Nominal values:  n = 1.3333 Fresh water n = 1.3334 Sea water

4.0

MUSAT-IIIA

4.1

Derivation of Mathematical Model for Refraction Correction

The mathematical algorithm to compensate for the refracted images of underwater points must address two problems. The first defining a local level surface in each of the various coordinate systems utilized by MUSAT-IIIA. The second problem is modifying the mathematics of the solution for water penetration.

The MUSAT-IIIA program contains preprocessors for blunder editing and for obtaining initial approximation for the solution. It has been assumed that these approximations are accurate enough to perform a rigorous solution taking into consideration the effect of water penetration.

The first mathematical problem addressed is the definition of the local level surface for each underwater point. Since the position of each point is not known, this is not a simple matter. In the preprocessing stage, the initial approximation for the position is determined. Once the preprocessing is complete, a coordinate transformation is set up for each underwater point and stored in the corresponding point file. This transformation is a conversion between the triangulation coordinate system and a local vertical coordinate system at each point.

Because of the earth curvature problems, and the problem of defining the local vertical, it is assumed that all water penetration triangulation will be performed in an earth centered coordinate system, and that the actual reduction will be in some cartesian system, either geocentric or local tangent.

As the points are processed, the positions of these points change

with each iteration of the solution. For a completely rigorous solution, during the point processing, the transformation matrix for each point is recomputed when the point position is updated for each iteration.

In order to take advantage of the geometry of light refraction in water, computation must be made in a local vertical coordinate system established for each point. The transformation to these coordinate systems, as discussed above, will be used to convert all coordinates to a local system. In the geometry of this local system, the modified collinearity equations can be established. The partial derivatives of the collinearity equations will then be converted to the triangulation coordinate system.

The following figure shows the geometry of the refracted light ray from an image point.

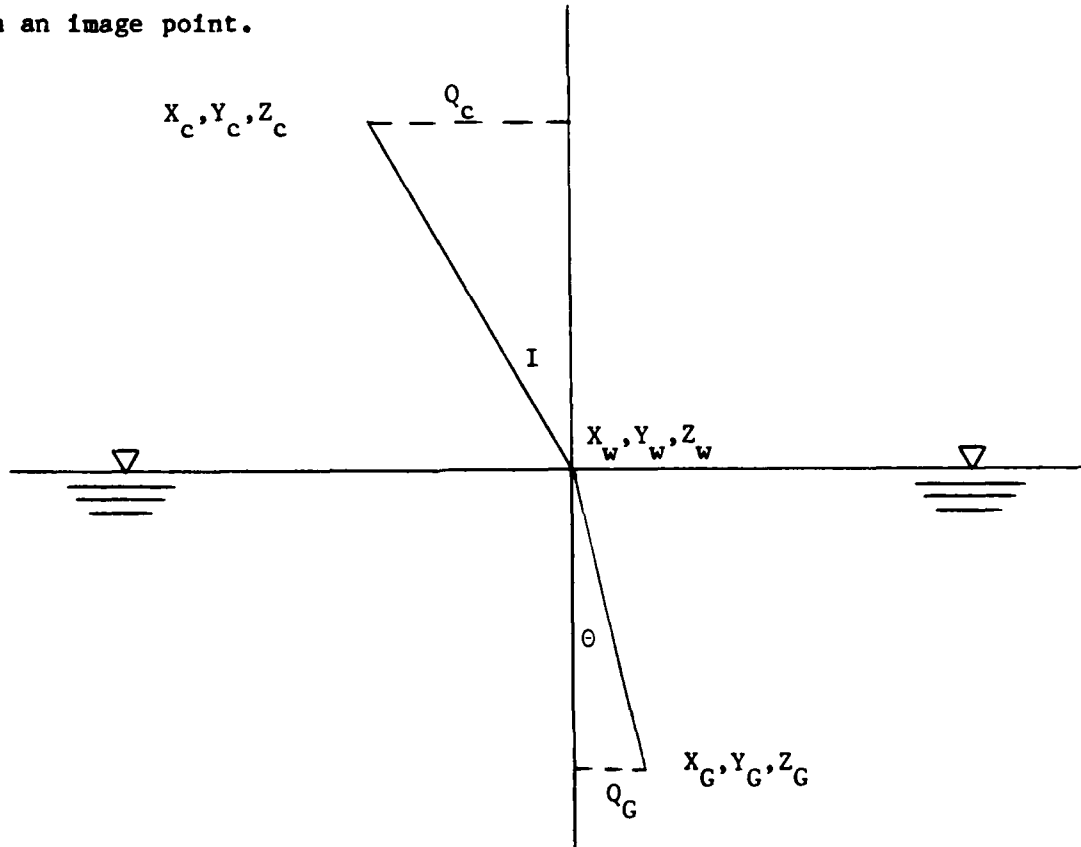


Figure 4.1 Refraction in a Bathymetric Point Image.

It is assumed for the solution that the elevation of the water,  $Z_w$  is a known quantity.

The collinearity condition does not hold for a submerged point due to the refraction imparted by the water column above the point. The general collinearity equations will be modified to reflect the geometry in Figure 4.1. The collinearity equations are written as:

$$\begin{bmatrix} X_w - X_C \\ Y_w - Y_C \\ Z_w - Z_C \end{bmatrix} = k R \begin{bmatrix} x - x_p \\ y - y_p \\ -f \end{bmatrix} \quad (4.1)$$

where,

$x, y$	- Image coordinates of a point
$x_p, y_p$	- Principal point offset
$f_i$	- Focal length
$R$	- Photo to ground rotation matrix
$S$	- Scale factor
$X_w, Y_w, Z_w$	- Coordinates of image ray/water surface intersection
$X_C, Y_C, Z_C$	- Camera station coordinates

However,  $X_w, Y_w$  are functions of  $X_C, Y_C, Z_C$ , and  $X_G, Y_G, Z_G$ . By differentiating the functions of  $X_w, Y_w$  with respect to the camera station and ground point coordinates; the variables  $X_w, Y_w$  can be eliminated from the equations. The partial derivatives of the projective equations will now be in terms of  $X_C, Y_C, Z_C, X_G, Y_G, Z_G$ , as they should be.

First, we define an axis Q such that the light ray lies in the QZ plane with the origin at the water surface. Viewing the light ray from above the XY plane, the ray would appear as in Figure 4.2. From Figure 4.1 and 4.2 we define the following:

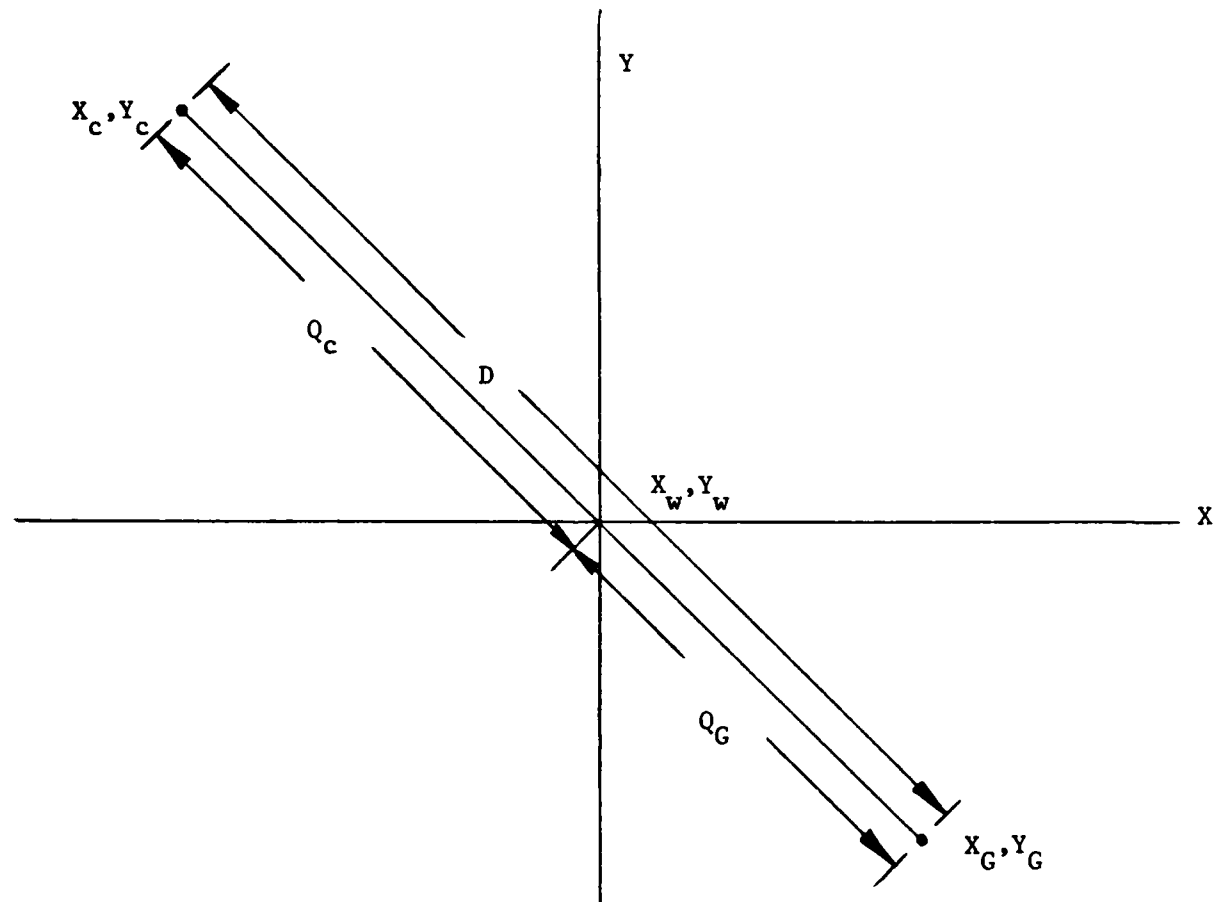


Figure 4.2 Top View of a Bathymetric Image Ray.

$$Q_C = ((X_C - X_W)^2 + (Y_L - Y_W)^2)^{1/2} \quad (4.2)$$

$$Q_G = ((X_W - X_G)^2 + (Y_W - Y_G)^2)^{1/2} \quad (4.3)$$

$$D = ((X_C - X_G)^2 + (Y_L - Y_G)^2)^{1/2} \quad (4.4)$$

It can be seen that,

$$D = Q_C + Q_G \quad (4.5)$$

and

$$Q_G = D - Q_C \quad (4.6)$$

From Figure 4.1,

$$\sin I = \frac{Q_C}{(Q_C^2 + (Z_W - Z_C)^2)^{1/2}} \quad (4.7)$$

$$\sin \theta = \frac{Q_G}{(Q_G^2 + (Z_G - Z_W)^2)^{1/2}} = \frac{D - Q_C}{((D - Q_C)^2 + (Z_G - Z_W)^2)^{1/2}} \quad (4.8)$$

Snell's Law of Refraction states:

$$\sin I = n \sin \theta \quad (4.9)$$

where,

n - Index of refraction

The function for combining all the parameters is then :

$$F = \sin \frac{Q_C}{(Q_C^2 + (z_w - z_C)^2)^{1/2}} - n \sin \frac{(D - Q_C)}{((D - Q_C)^2 + (z_G - z_w)^2)^{1/2}} = 0 \quad (4.10)$$

The function F can now be evaluated by iteration for the current values for  $x_w, y_w$ .

Let us define the collinearity equations as follows:

$$F_x = (x - x_p) + f \frac{R_{11} (x_w - x_C) + R_{12} (y_w - y_C) + R_{13} (z_w - z_C)}{R_{31} (x_w - x_C) + R_{32} (y_w - y_C) + R_{33} (z_w - z_C)} = 0 \quad (4.11)$$

$$F_y = (y - y_p) + f \frac{R_{21} (x_w - x_C) + R_{22} (y_w - y_C) + R_{23} (z_w - z_C)}{R_{31} (x_w - x_C) + R_{32} (y_w - y_C) + R_{33} (z_w - z_C)} = 0 \quad (4.12)$$

or,

$$F_x = (x - x_p) + f \frac{U}{W} = 0 \quad (4.13)$$

$$F_y = (y - y_p) + f \frac{V}{W} = 0 \quad (4.14)$$

In order to remove  $x_w, y_w$  from the partials, the chain rule must be applied in computing the following partials:

$$\frac{\partial X_w}{\partial X_C}, \frac{\partial X_w}{\partial Y_C}, \frac{\partial X_w}{\partial Z_C}, \frac{\partial Y_w}{\partial X_C}, \frac{\partial Y_w}{\partial Y_C}, \frac{\partial Y_w}{\partial Z_C}$$

$$\frac{\partial X_w}{\partial X_G}, \frac{\partial X_w}{\partial Y_G}, \frac{\partial X_w}{\partial Z_G}, \frac{\partial Y_w}{\partial X_G}, \frac{\partial Y_w}{\partial Y_G}, \frac{\partial Y_w}{\partial Z_G}$$

Differentiating the refraction function, F, using the chain rule, we have:

$$\frac{\partial F}{\partial X_C} = \frac{\partial F}{\partial Q_C} \frac{\partial Q_C}{\partial X_C} + \frac{\partial F}{\partial D} \frac{\partial D}{\partial X_C} \quad (4.15)$$

$$\frac{\partial F}{\partial Y_C} = \frac{\partial F}{\partial Q_C} \frac{\partial Q_C}{\partial Y_C} + \frac{\partial F}{\partial D} \frac{\partial D}{\partial Y_C} \quad (4.16)$$

$$\frac{\partial F}{\partial Z_C} = \frac{\partial F}{\partial Q_C} \frac{\partial Q_C}{\partial Z_C} + \frac{\partial F}{\partial D} \frac{\partial D}{\partial Z_C} \quad (4.17)$$

Similarly, we have:

$$\frac{\partial F}{\partial X_w} = \frac{\partial F}{\partial Q_C} \frac{\partial Q_C}{\partial X_w} + \frac{\partial F}{\partial D} \frac{\partial D}{\partial X_w} \quad (4.18)$$

$$\frac{\partial F}{\partial Y_w} = \frac{\partial F}{\partial Q_C} \frac{\partial Q_C}{\partial Y_w} + \frac{\partial F}{\partial D} \frac{\partial D}{\partial Y_w} \quad (4.19)$$

$$\frac{\partial F}{\partial Z_w} = \frac{\partial F}{\partial Q_C} \frac{\partial Q_C}{\partial Z_w} + \frac{\partial F}{\partial D} \frac{\partial D}{\partial Z_w} \quad (4.20)$$

We can combine these partials to form the required expressions. Specifically,

$$\frac{\partial X_w}{\partial X_C} = \frac{\frac{\partial F}{\partial X_C}}{\frac{\partial F}{\partial X_w}} \quad \frac{\partial X_w}{\partial Y_C} = \frac{\frac{\partial F}{\partial Y_C}}{\frac{\partial F}{\partial X_w}} \quad \frac{\partial X_w}{\partial Z_C} = \frac{\frac{\partial F}{\partial Z_C}}{\frac{\partial F}{\partial X_w}} \quad (4.21)$$

$$\frac{\partial X_w}{\partial X_G} = \frac{\frac{\partial F}{\partial X_G}}{\frac{\partial F}{\partial X_w}} \quad \frac{\partial X_w}{\partial Y_G} = \frac{\frac{\partial F}{\partial Y_G}}{\frac{\partial F}{\partial X_w}} \quad \frac{\partial X_w}{\partial Z_G} = \frac{\frac{\partial F}{\partial Z_G}}{\frac{\partial F}{\partial X_w}} \quad (4.22)$$

Similar construction results in the partials of  $Y_w$ , and  $Z_w$  with respect to the camera and ground point coordinates.

Now, taking the partial derivative of the collinearity equations with respect to camera station position, for example, and adding the contribution of the refraction function, the full partial becomes:

$$\frac{\partial F_x}{\partial X_C} = \frac{f}{w} \left( -R_{11} + \frac{u}{w} R_{31} \right) + \frac{\partial F_x}{\partial X_w} \frac{\partial X_w}{\partial X_C} + \frac{\partial F_x}{\partial Y_w} \frac{\partial Y_w}{\partial X_C} + \frac{\partial F_x}{\partial Z_w} \frac{\partial Z_w}{\partial X_C} \quad (4.23)$$

$$\frac{\partial F_y}{\partial X_C} = \frac{f}{w} \left( -R_{12} + \frac{v}{w} R_{31} \right) + \frac{\partial F_y}{\partial X_w} \frac{\partial X_w}{\partial X_C} + \frac{\partial F_y}{\partial Y_w} \frac{\partial Y_w}{\partial X_C} + \frac{\partial F_y}{\partial Z_w} \frac{\partial Z_w}{\partial X_C} \quad (4.24)$$

In the manner shown above, the discrepancy vector and the partial derivatives will be modified for all points which are under the water on each photograph. This will be accomplished by a modification of the routines which compute these discrepancies and partials, which are used universally throughout the program. The solution and its attendant error propagation of the errors through various output coordinate systems will remain valid.

## 4.2

Description of New Subroutines

Three new subroutines have been incorporated into the MUSAT-III A software package. These new routines deal specifically with the modifications made to the existing software to accommodate bathymetric image points. Should there be no requirement for this capability in any specified MUSAT-III A run, their inclusion will in no way affect the solution of the standard aerotriangulation problem.

4.2.1 SUBROUTINE UNWTR

SUBROUTINE: UNWTR

DATE WRITTEN June 1980

WRITTEN BY L. Peters Autometric. Inc.

LANGUAGE/MACHINE: FORTRAN / UNIVAC 1108 Exec 8

DESCRIPTION: This routine computes the coefficients of the collinearity condition equations for the submerged points. In this sense, the routine is functionally similar to the subroutine PTCOND in the existing MUSAT-IIIA software.

CALL LINE: CALL UNWTR ( ICOL, XWATER, XYZ, ISW )

INPUT: Thru the argument list -

ICOL - Column pointer to an image in the physical record

XYZ - Ground point coordinates in the triangulation system

ISW - Operational switch governing the use of the routine

OUTPUT: Thru the argument list -

XWATER(3) - Image ray/water surface intersection coordinates

Thru COMMON -

ATTCOE - Attitude coefficients of the condition equations

POSCOE - Position coefficients of the condition equations

GRNCOE - Ground coefficients of the condition equations

CONCOE - Constant coefficients of the condition equations

CALLED BY: LNK6C1, LNK6C2

METHOD: The first task addressed is to check the input coordinate system and perform the necessary coordinate transformations to reduce it to a geocentric coordinate system. This procedure includes transforming both the

coordinates and the orientation matrices as necessary. These coordinates are transformed into a local vertical system with its origin at the initial approximation for the submerged point's position as generated by the MUSAT preprocessors. We now have all the appropriate parameters, i.e., camera station parameters, ground point parameters, and associated orientation matrices in this local vertical system. At this point the value for the geographic height of the tidal elevation is also transformed to this system.

The next task is to compute the coordinates of the object space image ray - tidal surface intersection point. This is performed by invoking the second new subroutine, WATPNT, which will be discussed in detail in succeeding sections. The results of this routine are the X,Y coordinates of the intersection in the local vertical system. The "Z" coordinate is previously known as the tidal elevation. These local coordinates are then transformed back into geocentric coordinates to compute the constant coefficients of the collinearity condition equations in preparation for return to the calling program.

Computation of the partial derivatives of the collinearity equations now takes place. As discussed in the development of the mathematical model, the collinearity condition does not hold for submerged points. However, the partial derivatives of these equations can be modified to correct for the refraction of the image rays which invalidates this condition. The partials are computed as a function of the image ray - water surface intersection point. In this manner, the submerged point can be incorporated into the standard aerotriangulation problem.

The partial derivatives for the submerged points are computed in the local vertical system and then transformed into the original triangulation system in preparation for solution of the triangulation problem. These partial derivatives are described in detail in Section 4.1 of this report. At this point control returns to the calling routine for continuation of the normal program processing.

**LIMITATIONS:** None

**COMMON BLOCKS:** /FRDATA/ /GNDATA/ /WATER/  
/COEFPT/ /IDX/ /FLAGS/  
/DATAB3/ /AXES/ /TAPES/

**OPTIONS:** None

**SUBROUTINES**

REFERENCED: RTFRM4, PLHXY1, WATPNT, MPYAB3, ADDMT3

4.2.2 SUBROUTINE WATPNT

SUBROUTINE: WATPNT

DATE WRITTEN: May 1980

WRITTEN BY: L. Peters.

LANGUAGE/MACHINE: FORTRAN / UNIVAC 1108 Exec 8

DESCRIPTION: This subroutine computes the coordinates of the image ray/water surface intersection for a bathymetric image point.

CALL LINE: CALL WATPNT ( XCAM, XGRD, TIDE, WAT, ICOL, J )

INPUT: Thru the argument list -

XCAM - Camera station coordinates

XGRD - Ground point coordinates

TIDE - Height of water surface

ICOL - Column pointer to an image in the physical record

J - Internal frame identifier

OUTPUT: XWAT - Image ray/water surface intersection coordinates

CALLED BY: UNWTR

METHOD: The maximum value for the refraction angle is defined by

$$\theta_{\max} = \sin^{-1} \frac{1}{n} ;$$

and the minimum value is 0. A binary interpolation is performed to compute the value of the refraction angle for each image ray. Knowing the refraction angle, the incidence angle, I, can be computed using Snell's Law. The image ray/water surface intersection coordinates can be computed from :

$$x_w = x_c - \frac{(x_c - x_g)(z_c - z_w) \tan I}{((x_c - x_g)^2 + (y_c - y_g)^2)^{1/2}}$$

$$y_w = y_c - \frac{(y_c - y_g)(z_c - z_w) \tan I}{((x_c - x_g)^2 + (y_c - y_g)^2)^{1/2}}$$

LIMITATIONS: None

COMMON BLOCKS: /FLAGS/ /IDX/ /TAPES/

OPTIONS: None

SUBROUTINES  
REFERENCED: NONE

#### 4.2.3 SUBROUTINE RTLCGC

**SUBROUTINE:** **RTLCGC**

DATE WRITTEN: June 1980

WRITTEN BY: L. Peters

LANGUAGE/MACHINE: FORTRAN / UNIVAC 1108 Exec 8

**DESCRIPTION:** This subroutine computes the local to geocentric rotation for each bathymetric point.

**CALL LINE:** **CALL RLTCGC**

**INPUT:** Thru ITAPE2 -

NREC	- Number of records in subrecord
IPNTER	- Pointer to beginning column of subrecord
JJ	- Total number of columns in subrecord
RECORD	- Ground, image, elimination, addition, and camera distance subrecords

OUTPUT: Thru ITAPE2 =

**IWATRT** - Local to geocentric rotation matrix for the bathymetric point

CALLED BY: **LINK5A**

**METHOD:** See MUSAT Program Documentation for subroutine  
RTFRM6.

**LIMITATIONS:** None

COMMON BLOCKS: /COUNTR/ /TAPES/ /FLAGS/

OPTIONS:  None

## SUBROUTINES

## REFERENCED: REF

**SUBROUTINES  
REFERENCED:** RTFRM6

## 4.3

DICTIONARY OF NEW COMMON BLOCKS - MUSAT-IIIA

## COMMON /INDX/ SN

<u>VARIABLE</u>	<u>TYPE DESCRIPTION</u>	
SN	Real	Index of refraction of the water body

## COMMON /WATER/ IREC, IWATPT(11,50)

<u>VARIABLE</u>	<u>TYPE DESRIPTION</u>	
IREC	Integer	Number of point records
IWATPT(1,I)	Integer	Point ID
IWATPT(2,I)	Integer	Bathymetric flag
IWATPT(3-11,I)	Integer	Local to geocentric rotation matrix for a bathymetric point

## 5.0

MODIFICATION OF AS-11AM FRAME SOFTWARE  
FOR BATHYMETRIC COMPILATION

In addition to the capability to triangulate bathymetric points using the MUSAT programs, the capability to compile bathymetric points on the AS-11AM using conventional frame imagery was provided. The section develops the mathematics involved in the computation of the true coordinates of bathymetric points.

## 5.1

## COMPUTATION OF TRUE COORDINATES FOR BATHYMETRIC POINTS

All computations for the correction of measured model coordinates are performed in the model coordinate system. The tide elevation for each frame, input in a geographic coordinate system is transformed into model space by applying the appropriate transformation coefficients. We can now define the following notation:

$Bx_1, By_1, Bz_1$       - Model coordinates of the left and right camera stations respectively.

$Bx_2, By_2, Bz_2$

$Zw_1, Zw_2$       - Model space height of water surface on left and right frames respectively.

$n$       - Index of refraction of water. (Assumed equivalent on both frames)

$X_p, Y_p, Z_p$       - Model coordinates of a measured bathymetric point.

$Xw_1, Yw_1$   
 $Xw_2, Yw_2$       - Model coordinates of image ray/water surface intersection on left and right frames respectively.

$X_T, Y_T, Z_T$       - True model coordinates of a measured bathymetric point.

The first step in computing the true model coordinates is to compute the image ray/water surface intersection for each frame. We have:

$$X_{W1} = Bx_1 + (Bz_1 - Zw_1) \frac{(X_p - Bx_1)}{(Bz_1 - Z_p)} \quad (5.1)$$

$$Y_{W_1} = B_{Y_1} + (B_{Z_1} - Z_{W_1}) \frac{(Y_P - B_{Y_1})}{(B_{Z_1} - Z_P)} \quad (5.2)$$

$$x_w_2 = b x_2 + (b z_2 - z_w_2) \frac{(x_p - b x_2)}{(b z_2 - z_p)} \quad (5.3)$$

$$Y_{w2} = Bz_2 + (Bz_2 - Zw_2) \frac{(Y_p - By_2)}{(Bz_2 - Z_p)} . \quad (5.4)$$

Next, the angles of incidence and refraction of the image rays are computed.

Let,

$$D_1 = ((Bx_1 - X_{w1})^2 + (By_1 - Y_{w1})^2)^{1/2} \quad (5.5)$$

$$D_2 = ((Bx_2 - X_{w2})^2 + (By_2 - Y_{w2})^2)^{1/2} \quad (5.6)$$

The angles of incidence are, then :

$$I_1 = \tan^{-1} \left[ \frac{D_1}{Bz_1 - Zw_1} \right] \quad (5.7)$$

$$I_2 = \tan^{-1} \left[ \frac{D_2}{Bz_2 - Zw_2} \right] \quad (5.8)$$

The angles on refraction due to the water surface are now :

$$\theta_1 = \sin^{-1} \left[ \frac{\sin I_1}{n} \right] \quad (5.9)$$

$$\theta_2 = \sin^{-1} \left[ \frac{\sin I_2}{n} \right] \quad (5.10)$$

The true coordinates of the bathymetric are defined by the intersection of the underwater image rays of a bathymetric point from each frame.

$$\begin{bmatrix} X_T - X_{w1} \\ Y_T - Y_{w1} \\ Z_T - Z_{w1} \end{bmatrix} = k \begin{bmatrix} r_1 \\ r_2 \\ r_3 \end{bmatrix} \quad (5.11)$$

$$\begin{bmatrix} X_T - X_{w2} \\ Y_T - Y_{w2} \\ Z_T - Z_{w2} \end{bmatrix} = k \begin{bmatrix} r'_1 \\ r'_2 \\ r'_3 \end{bmatrix} \quad (5.12)$$

Now,

$$(X_T - X_{w1}) = (r_1/r_3) (Z_T - Z_{w1}) = r_{13} Z_T - r_{13} Z_{w1} \quad (5.13)$$

$$(Y_T - Y_{w1}) = (r_2/r_3) (Z_T - Z_{w1}) = r_{23} Z_T - r_{23} Z_{w1} \quad (5.14)$$

$$(X_T - X_{w2}) = (r'_1/r'_3) (Z_T - Z_{w2}) = r'_{13} Z_T - r'_{13} Z_{w2} \quad (5.15)$$

$$(Y_T - Y_{w2}) = (r'_2/r'_3) (Z_T - Z_{w2}) = r'_{23} Z_T - r'_{23} Z_{w2} \quad (5.16)$$

In matrix form,

$$\begin{bmatrix} 1 & 0 & -r_{13} \\ 1 & 0 & -r'_{13} \\ 0 & 1 & -r_{23} \\ 0 & 1 & -r'_{23} \end{bmatrix} \begin{bmatrix} X_T \\ Y_T \\ Z_T \end{bmatrix} = \begin{bmatrix} X_{w1} - r_{13} Z_{w1} \\ X_{w2} - r'_{13} Z_{w2} \\ Y_{w1} - r_{23} Z_{w1} \\ Y_{w2} - r'_{23} Z_{w2} \end{bmatrix} = \begin{bmatrix} a_1 \\ a'_1 \\ a_2 \\ a'_2 \end{bmatrix} \quad (5.17)$$

$$r_{13} = \tan \theta_1 (X_{w1} - Bx_1) / -D_1 \quad (5.17a)$$

$$r_{23} = \tan \theta_1 (Y_{w1} - By_1) / -D_1 \quad (5.17b)$$

$$r'_{13} = \tan \theta_2 (X_{w2} - Bx_2) / -D_2 \quad (5.17c)$$

$$r'_{23} = \tan \theta_2 (Y_{w2} - By_2) / -D_2 \quad (5.17d)$$

The normals are,

$$\begin{bmatrix} 2 & 0 & -(r_{13} + r'_{13}) \\ 0 & 2 & -(r_{23} + r'_{23}) \\ -(r_{13} + r'_{13}) & -(r_{23} + r'_{23}) & (r_{13}^2 + r'_{13}^2 + r_{23}^2 + r'_{23}^2) \end{bmatrix} \begin{bmatrix} X_T \\ Y_T \\ Z_T \end{bmatrix} = \begin{bmatrix} a_1 + a'_1 \\ a_2 + a'_2 \\ Q \end{bmatrix}$$

where,

$$Q = -(r_{13}a_1 + r'_{13}a'_1 + r_{23}a_2 + r'_{23}a'_2)$$

Let,

$$c_{13} = -(r_{13} + r'_{13}) \quad (5.18)$$

$$c_{23} = -(r_{23} + r'_{23}) \quad (5.19)$$

$$c_{33} = (r_{13}^2 + r'_{13}^2 + r_{23}^2 + r'_{23}^2) \quad (5.20)$$

$$c_1 = a_1 + a'_1 \quad (5.21)$$

$$c_2 = a_2 + a'_2 \quad (5.22)$$

$$c_3 = 0 \quad (5.23)$$

Solving the system, we have the true coordinates of the bathymetric point.

$$z_T = \frac{c_3 - \frac{1}{2}(c_{13}c_1 + c_{23}c_2)}{c_{33} - \frac{1}{2}(c_{13}^2 + c_{23}^2)} \quad (5.24)$$

$$x_T = \frac{1}{2}(c_1 - c_{13}z_T) \quad (5.25)$$

$$y_T = \frac{1}{2}(c_2 - c_{23}z_T) \quad (5.26)$$

## 6.0

### TESTING AND EVALUATION OF MODIFIED MUSAT PROGRAMS AND AS-11 SOFTWARE

This section presents the results of the operational testing and evaluation of the modified MUSAT aerotriangulation program, and the modified AS-11 compilation software. Due to time constraints, the testing of the modified MUSAT-IIIA program is not yet complete and therefore its test results are not included in this report.

#### TESTING & EVALUATION - MUSAT

According to Contract Section 4.2.2 Quality Assurance, the following conditions will govern the Testing & Evaluation of the modified software:

"To verify the validity and accuracy of the modified programs, the contractor shall perform a photogrammetric block aerotriangulation using reference photography and associated numerical data provided by the government. A minimum of 10 photographs will be used for this test. Image points with known ground coordinates will be carried as unknowns in the solution. At least half of the image points used shall be subsurface points. The accuracy goal for these modified programs will be to achieve photograph residuals with a root-mean-square error of 15 micrometers with calm sea conditions".

The testing and evaluation of the programs was performed by DMAHTC and Autometric personnel at DMAHTC.

The test data consists of a 10 photograph strip of conventional frame photography of the Cayman Islands. The strip was marked and measured by DMAHTC personnel, and triangulated, without regard to the effects of refraction, using the production MUSAT-IIA, and MUSAT-IIIA programs. There

were a total of 98 ground points measured on the film. Of these, 12 were bathymetric points. All of the bathymetric points were located on four frames of the 10 frame strip. It must be noted that the strip, without the refraction model in place, would not triangulate within the standard convergence criteria of differential rotation and differential translation, for either MUSAT program. The convergence criteria were relaxed by one order of magnitude in order to allow convergence of the solution.

There are several factors which may have contributed to the failure of this strip triangulation solution to converge. The first has to do with the geodetic data used to control the strip. The control data provided was believed to be of first order quality. However, after analyzing the behavior of the control points during the triangulation solution, it appears that the control may not be of first order quality. Secondly, the control points were not easily identifiable on the photographs. The control points consisted of monumented horizontal and vertical marks. None of the control was paneled. Therefore, the inherent error in the identification of the control points during the point mensuration is not insignificant.

The standard error of the point mensuration is not well known. Various values were assigned for the standard error of the measured image coordinates during the testing phase. As suggested previously in this report, Autometric has suggested assigning an image coordinate measurement standard error of 1.5 to 2 times the normal value to measured bathymetric points. The adopted value for all measured image coordinates was 10 microns in x and y.

Notwithstanding these problems, this data set was used for the testing.

The following guidelines were used in the Testing & Evaluation of the modified MUSAT programs:

1. Run a standard production (non-bathymetric) data set using the production version of MUSAT and the modified version of MUSAT exercising all input and output options.
2. Run a bathymetric data set through the modified MUSAT program exercising all input and output options.
3. Analyze the results of the bathymetric point triangulation as compared with the production program triangulation with no refraction correction.
4. Analyze the computed bathymetric heights (depths) as compared to sounding data obtained using standard bathymetric techniques. Also compare to hand calculation of estimated depth change due to water column.

#### RESULTS OF TESTING - MUSAT-IIA

The first two items in the testing guidelines are designed to verify that all standard program operation options are still addressable. These options include such things as: variations of the input coordinate system, pre-processed or unprocessed plate measurements, card output, etc. All of the options were verified.

The results of the third item in the testing guidelines are

summarized in Tables 6-1 through 6-10.

The analyses presented here in table form are the standard statistical reports generated by a MUSAT program run. Tables 6-1 and 6-5 show the analysis of the adjusted camera station positions for standard MUSAT-II program and the modified MUSAT-II program. The sample size denotes the number of camera stations adjusted during the program execution. The next entry, Sum of Differences, gives the accumulated sums of the differences between the initial estimates for the camera station positions and the adjusted camera station positions. Note the improvement in the position analysis for the modified program versus the standard program. This implies the the modified program more accurately represents the geometric characteristics of the imaging process than the standard program; as is expected.

Inspection of Tables 6-2 and 6-6 show only a slight improvement for the camera attitudes from the modified program. Again, only four of the frames in the strip had water points imaged.

Tables 6-3 and 6-7 show the ground point analysis for both programs. The ground points included in the analysis are only the control points for the triangulation run. There were a total of 7 horizontal control points and a total of 35 vertical control points in the strip. The differences again are the differences between the given control point coordinates and the adjusted values of control point coordinates. Table 6-7 shows a slight improvement in the Latitude and Longitude components for the control points. As expected, the greatest improvement occurs in the Height components. This is due to the fact that the refraction effects imparted by the water column above a point has its greatest effect on the computed height (depth) of a point. It is interesting to note that none of the control points showing a maximum value for the difference is a bathymetric point.

Tables 6-4 and 6-8 show the computed RMS plate residuals for all frames in the strip. The Tables differentiate between points which were included in the triangulation solution and those which were not. The most notable entries in Table 6-4 are the values for the y-coordinate residuals of points on Frames 841 to 845. These are the only frames in the strip which contained bathymetric points. Table 6-8 show the improvements in the point residuals for Frames 841 to 845 after the refraction model has been applied. The effects of refraction alone do not account for the large values for the y-coordinate residuals in the standard program. Table 6-4 shows that the y-coordinate residuals for all frames are approximately twice the values of the x-coordinate residuals. This implies some sort of systematic problem in either point mensuration or in the application of image coordinate refinements.

The first column of Table 6-9 shows the values for the geocentric coordinates of the bathymetric points computed by the standard MUSAT-IIA program before correction for refraction. The approximate coordinates for the bathymetric points can be computed if the assumption is made that all of the corrections to the computed coordinates occur in the Z component. Given the adjusted camera station coordinates and ground point coordinates from the standard run, the direction numbers and angles of incidence of the image rays with the water surface are computed. The coordinates of the intersection of the image ray and the water surface are also computed. The approximate change in height is computed by applying the refraction angle to the direction numbers and intersecting the underwater image rays for point. These computed approximate positions are tabulated in the second column of Table 6-9. The actual computed positions from the modified MUSAT-IIA program are tabulated in the third column of Table 6-9.

Table 6.1

Camera Station Position Analysis Standard MUSAT-IIA  
No Refraction Correction  
(Degrees, Minutes, Seconds)

	Latitude			Longitude			Elev. (M)
Sample Size	10			10			10
Sum of Differences	-0	0	.281	0	0	5.296	104.71
Mean Value of Differences	-0	0	.028	0	0	.530	10.47
RMS of Differences	0	0	.140	0	0	.830	27.30
Standard Deviation from Mean	0	0	.144	0	0	.674	26.58
Maximum Difference	-0	0	.247	0	0	1.543	66.72
Camera with Max. Difference	842			843			846

Table 6.2

Camera Station Attitude Analysis Standard MUSAT-IIA  
No Refraction Correction  
(Degrees, Minutes, Seconds)

	X-Tilt	Y-Tilt	Heading
Sample Size	10	10	10
Sum of Differences	-0 08 46.908	-1 22 2.182	-0 0 1.033
Mean Value of Differences	-0 0 52.691	-0 08 12.218	-0 0 .103
RMS of Differences	0 2 14.428	0 12 30.847	0 0 .792
Standard Deviation from Mean	0 2 10.360	0 09 57.674	0 0 .828
Maximum Difference	-0 3 42.153	-0 23 50.092	0 0 1.955
Camera with Max. Difference	845	846	842

Table 6.3

Ground Point Analysis Standard MUSAT-IIA  
No Refraction Correction  
(Degrees, Minutes, Seconds)

	Latitude	Longitude	Elev. (M)
Sample Size	7	7	35
Sum of Differences	0 0 .035	-0 0 .120	4.84
Mean Value of Differences	0 0 .005	-0 0 .017	.14
RMS of Differences	0 0 .035	0 0 .050	4.87
Standard Deviation from Mean	0 0 .081	0 0 .050	4.94
Maximum Difference	0 0 .081	-0 0 .123	-9.98
Point with Max. Difference	1103	1215	1104

Table 6.4

Plate Residuals Standard MUSAT-IIA  
No Refraction Correction (MM)

Frame	837	838	839	840	841	842	843	844	845	846
RMS of Trig.										
Points - x	.004	.005	.004	.003	.006	.008	.008	.009	.008	.006
RMS of Trig.										
Points - y	.007	.012	.013	.017	.016	.016	.015	.010	.009	.006
RMS of Points										
Not Trig. - x	.000	.000	.000	.000	.005	.020	.030	.013	.000	.000
RMS of Non-										
Trig. Pts. - y	.000	.000	.000	.000	.139	.138	.108	.203	.000	.000
Rms of All										
Points - x	.004	.005	.004	.003	.006	.010	.013	.010	.008	.006
RMS of All										
Points - y	.007	.012	.013	.017	.033	.043	.040	.068	.009	.006
Frame With Max. RMS Trig. Pts.					****					
Frame With Max. RMS Non- Trig. Points						****				
Frame With Max. RMS All Pts							****			

Table 6.5

Camera Station Position Analysis Modified MUSAT-IIA  
Refraction Correction Applied  
(Degrees, Minutes, Seconds)

	Latitude	Longitude	Elev. (M)
Sample Size	10	10	10
Sum of Differences	-0 0 .103	0 0 4.798	95.53
Mean Value of Differences	-0 0 .100	0 0 .480	9.55
RMS of Differences	0 0 .144	0 0 .805	25.00
Standard Deviation from Mean	0 0 .151	0 0 .682	24.36
Maximum Difference	-0 0 .259	0 0 1.623	64.54
Camera with Max. Difference	844	844	846

Table 6.6

Camera Station Attitude Analysis Modified MUSAT-IIA  
Refraction Correction Applied  
(Degrees, Minutes, Seconds)

	X-Tilt			Y-Tilt			Heading		
Sample Size	10			10			10		
Sum of Differences	-0	11	24.831	-1	17	4.377	-0	0	.433
Mean Value of Differences	-0	1	4.483	-0	7	42.438	-0	0	.044
RMS of Differences	0	2	8.940	0	13	36.180	0	0	.454
Standard Deviation from Mean	0	1	55.159	0	11	48.913	0	0	.476
Maximum Difference	-0	3	55.337	-0	24	48.507	0	0	.947
Camera with Max. Difference	845			846			842		

Table 6.7

Ground Point Analysis Modified MUSAT-IIA  
Refraction Correction Applied  
(Degrees, Minutes, Seconds)

	Latitude	Longitude	Elev. (M)
Sample Size	7	7	35
Sum of Differences	0 0 .010	-0 0 .111	- .66
Mean Value of Differences	0 0 .001	-0 0 .016	- .02
RMS of Differences	0 0 .040	0 0 .042	4.46
Standard Deviation from Mean	0 0 .043	0 0 .042	4.52
Maximum Difference	0 0 .070	-0 0 .068	-9.79
Point with Maximum Difference	1210	1109	1104

Table 6.8

Plate Residuals Modified MUSAT-IIA  
Refraction Correction Applied (MM)

Frame	837	838	839	840	841	842	843	844	845	846
RMS of Trig.										
Points - x	.004	.005	.004	.002	.004	.003	.004	.007	.006	.004
RMS of Trig.										
Points - y	.007	.011	.013	.015	.013	.011	.008	.004	.006	.005
RMS of Points										
Not Trig. - x	.000	.000	.000	.000	.005	.004	.002	.001	.000	.000
RMS of Non-										
Trig. Pts. - y	.000	.000	.000	.000	.141	.101	.002	.002	.000	.000
Rms of All										
Points - x	.004	.005	.004	.002	.004	.003	.004	.007	.006	.004
RMS of All										
Points - y	.007	.011	.013	.015	.032	.031	.008	.004	.006	.005
Frame With										
Max. RMS										
Trig. Pts.					****					
Frame With										
Max. RMS Non-										
Trig. Points						****				
Frame With										
Max. RMS All Pts								****		

Table 6.9

Comparison of Computed Bathymetric  
Geocentric Point Coordinates (M)

Point Number	MUSAT-IIA		Predicted Pos. Approx.	MUSAT-IIA Refraction
	No-Refrac.			
1047*	X	907446.7	907446.7	907450.4
	Y	-5951412.7	-5951412.5	-5951413.1
	Z	2099645.1	2099643.9	2099644.8
1056*	X	904464.1	904464.1	904464.7
	Y	-5952644.9	-5950278.3	-5952644.5
	Z	2097470.7	2097470.2	2097466.9
1042	X	911407.6	911405.7	911413.8
	Y	-5950277.0	-5950277.4	-5950279.9
	Z	2101164.5	2101162.6	2101164.7
1043	X	911393.6	911393.9	911400.0
	Y	-5949788.3	-5949788.4	-5949795.4
	Z	2102554.4	2102558.8	2102555.2
1044	X	910095.7	910096.4	910101.4
	Y	-5949944.2	-5949944.9	-5949940.9
	Z	2102655.6	2102663.6	2102656.6
1046	X	909448.2	909448.2	909453.9
	Y	-5951347.2	-5951347.2	-5951346.9
	Z	2098993.3	2098992.4	2098992.1
1049	X	907741.1	907740.2	907745.3
	Y	-5950406.7	-5950406.7	-5950409.4
	Z	2102371.8	2102382.8	2102374.6
1050	X	907876.0	907878.2	907880.4
	Y	-5950185.4	-5950187.2	-5950190.0
	Z	2102946.5	2102963.9	2102950.1
1051	X	905938.3	905938.9	905940.3
	Y	-5950307.8	-5950308.2	-5950302.6
	Z	2103416.2	2103422.9	2103418.7
1052	X	904873.0	904871.9	904874.1
	Y	-5950709.9	-5950709.8	-5950706.3
	Z	2102743.1	2102722.8	2102745.1

Table 6.9 (cont.)

	X	904824.7	904819.1	904826.4
1053**	Y	-5950463.2	-5950459.6	-5950462.7
	Z	2103484.2	2103490.2	2103488.2
	X	903378.8	903379.0	903378.3
1057	Y	-5950270.4	-5950270.7	-5950272.0
	Z	2104631.8	2104636.4	2104636.3

\* - Point not triangulated.

\*\* - Point is a vertical control point.

TESTING & EVALUATION - AS-11 SOFTWARE

According to Contract Paragraph F.2 (Modified):

"Acceptance or rejection of the software program shall be determined using the following criterion. The positions of points obtained using the software program developed under this contract modification shall not differ significantly from the positions obtained for the same points using the modified MUSAT software program developed under this contract. The contours obtained by the AS-11AM using the delivered software program shall compare favorably with those of the same area obtained by standard bathymetric means.

The test data consisted of a three photograph strip of conventional frame photography of St. Thomas, USVI. The strip was triangulated using the modified MUSAT-IIA program. The resulting triangulation data was used as input to the modified FCA Frame Compilation software on the AS-11. The following guidelines were used in the Testing & Evaluation of the modified AS-11 compilation software:

1. Obtain MUSAT-IIA or MUSAT-III A triangulation data and the accompanying film for the stereomodels.
2. Perform a stereomodel setup using the results of the MUSAT triangulation, and verify all standard FCA options.
3. Collect geomorphic (point) and profile data.
4. Analyze the collected geomorphic data as compared to the triangulation results of the MUSAT run.
5. Analyze the collected profile data as compared to sounding data

collected using standard techniques (NOS sounding sheets).

RESULTS OF TESTING - AS-11 SOFTWARE

The St. Thomas triangulation data from the MUSAT run was used as input to the modified AS-11 program. A model setup was performed. After the interior orientation was performed, the stereomodel set up satisfactorily, that is with a minimum of y-parallax. Photo coordinates on the AS-11 were recoverable to within 10-15 microns of their final values from the MUSAT run.

The comparison of the geomorphic data collection and the MUSAT triangulation shows differences in the position vectors of 0.5 - 1.6 meters; with the greatest difference being in the Z component. Some of the factors affecting the ability to perceive stereo underwater are: "shimmer" of the surface due to unfavorable sun angle, reflectance characteristics of the bottom, and the inability of the cartographer to recognize when x-parallax has been completely removed, i.e when the "dot" is on the bottom.

